Deformation structures resulting from anisotropy during high-strain deformation of ice 1h with initial CPO

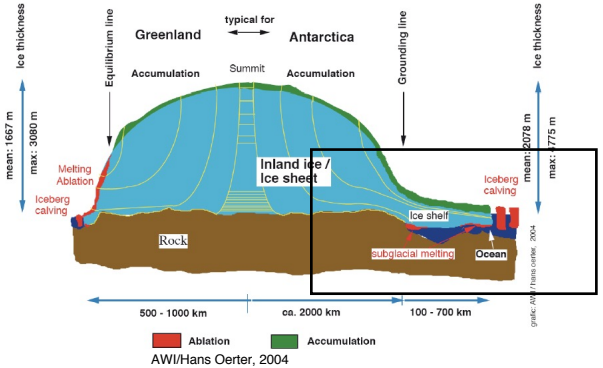
Tamara de Riese[1]

Paul Bons[1], Enrique Gomez-Rivas[2], Albert Griera[3], Maria-Gema Llorens[4], Ilka Weikusat[1,5]

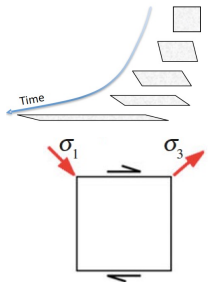
(1) Department of Geosciences, Eberhard Karls University Tübingen, Germany (2) Department of Mineralogy, Petrology and Applied Geology, University of Barcelona, Barcelona, Spain (3) Departament de Geologia, Universitat Autònoma de Barcelona, Barcelona, Spain , (4) Institute of Earth Sciences Jaume Almera (ICTJA-CSIC), Barcelona, Spain. (5) Alfred Wegener Institute Helmholtz Centre for Polar and Marine Research, Bremerhaven, Germany. *Email:* tamara.de-riese@uni-tuebingen.de

Flow of ice

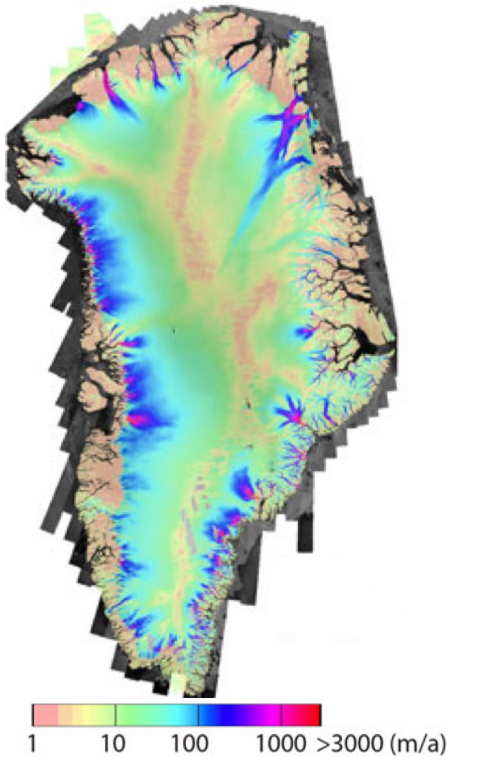
- Surface velocities of the Greenland ice sheet indicate heterogeneous deformation
- The flow of ice is controlled by the highly anisotropic rheology of ice 1h
- During flow the viscoplastic anisotropy leads the development of a crystallographic preferred orientation (CPO)
- High anisotropy of ice: basal plane 60 to 80 times softer than other slip planes (Duval et al., 1983)
- Ice 1h has therefore the properties to induce strain localisation



AWI/Hans Oerter, 2004



Flow varies within the ice sheet: Flow at flanks is dominated by **simple shear**



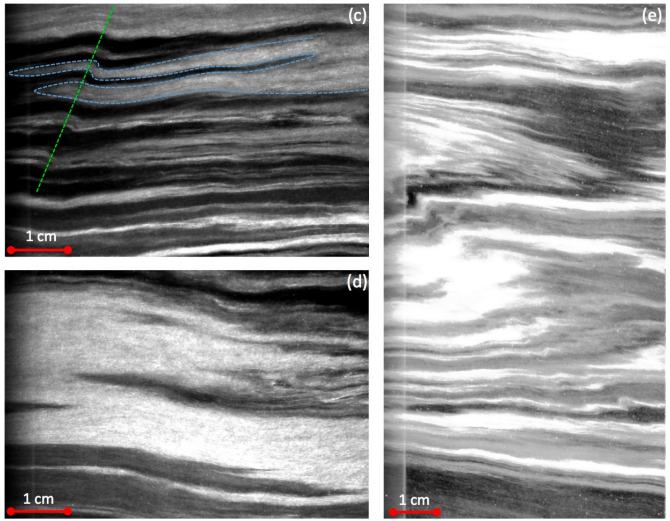
Measured ice flow velocities in Greenland. From Joughin et al., 2018

Joughin, I. A. N., Smith, B. E., & Howat, I. M. (2018). A complete map of Greenland ice velocity derived from satellite data collected over 20 years. *Journal of Glaciology*, *64*(243), 1-11.

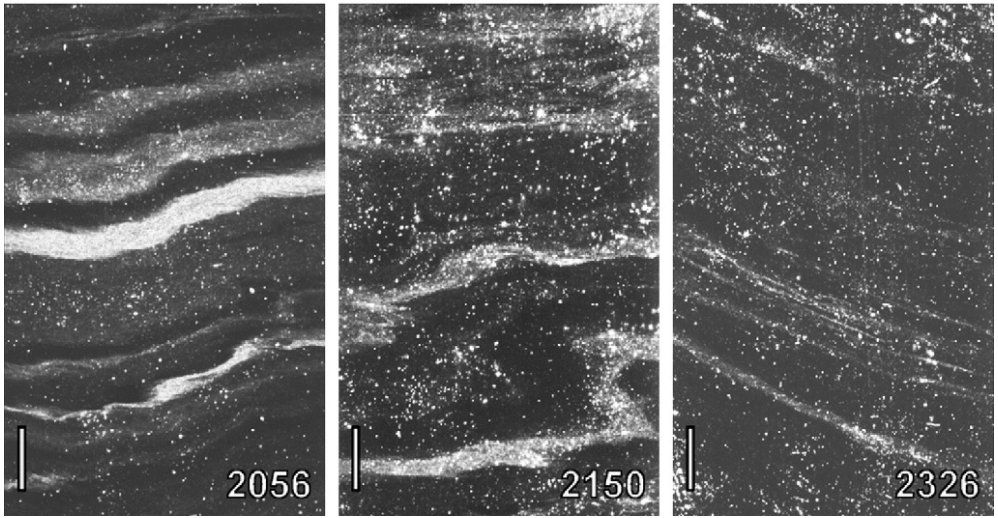
Duval, P., Ashby, M. F., & Anderman, I. (1983). Rate-controlling processes in the creep of polycrystalline ice. *The Journal of Physical Chemistry*, *87*(21), 4066-4074.

de Riese, T., Bons, P. D., Gomez-Rivas, E., Griera, A., Llorens, M.-G., and Weikusat, I.: Deformation structures resulting from anisotropy during high-strain deformation of ice 1h with initial CPO, EGU General Assembly 2021, online, 19–30 Apr 2021, EGU21-10209, https://doi.org/10.5194/egusphere-egu21-10209, 2021.

Deformation structures in ice



Cloudy bands in NEEM ice core. Jansen et al., 2016. Fig 2

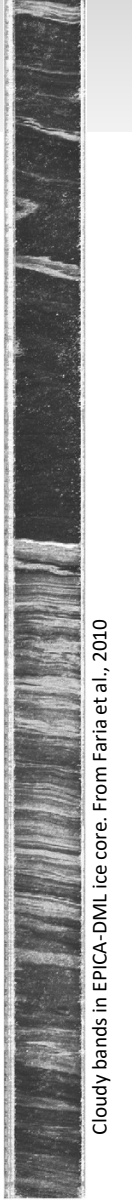


Cloudy bands in EPICA-DML ice core. From Faria et al., 2010. Fig.1)

- Ice shows localisation structures on the small scale
- No reason to assume it only occurs on the small scale

Faria, S. H., Freitag, J., & Kipfstuhl, S. (2010). Polar ice structure and the integrity of ice-core paleoclimate records. *Quaternary Science Reviews*, *29*(1-2), 338-351.
Jansen, D., Llorens, M. G., Westhoff, J., Steinbach, F., Kipfstuhl, S., Bons, P. D., ... & Weikusat, I. (2016). Small-scale disturbances in the stratigraphy of the NEEM ice core: observations and numerical model simulations. *The Cryosphere*, *10*(1), 359-370.

de Riese, T., Bons, P. D., Gomez-Rivas, E., Griera, A., Llorens, M.-G., and Weikusat, I.: Deformation structures resulting from anisotropy during high-strain deformation of ice 1h with initial CPO, EGU General Assembly 2021, online, 19–30 Apr 2021, EGU21-10209, https://doi.org/10.5194/egusphere-egu21-10209, 2021.



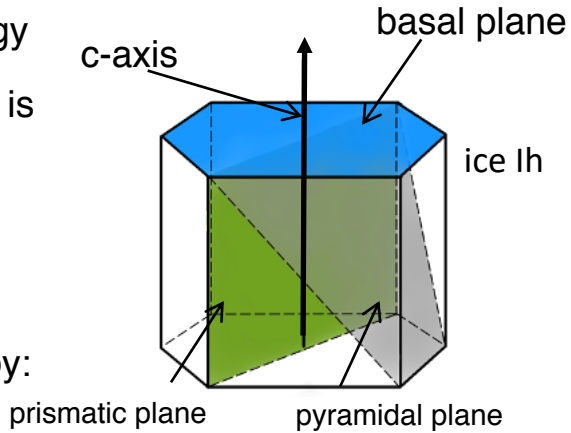
Aims

- Simulate the deformation of intrinsically anisotropic ice 1h with an initial single maximum crystallographic preferred orientation in dextral simple shear up to very high strains
- Investigate the role of material markers such as cloudy bands
- What kind of deformation behaviours can be expected?
- When do we reach a steady-state in fabric and stress evolution, localisation behaviour, etc.?

de Riese, T., Bons, P. D., Gomez-Rivas, E., Griera, A., Llorens, M.-G., and Weikusat, I.: Deformation structures resulting from anisotropy during high-strain deformation of ice 1h with initial CPO, EGU General Assembly 2021, online, 19–30 Apr 2021, EGU21-10209, https://doi.org/10.5194/egusphere-egu21-10209, 2021.

Modelling approach: VPFFT + ELLE

- Viscoplastic full-field formulation (VPFFT) coupled with modelling platform ELLE (Lebensohn, 2001; Griera et al., 2013; Llorens et al., 2016, de Riese et al., 2019 for details)
- Approach is able to achieve very high strains and include anisotropic rheology
- Nonlinear viscous rate-dependent approach, where viscoplastic deformation is assumed to be accommodated by dislocation glide on 3 slip systems (basal, prismatic and pyramidal), no recrystallisation
- Different critical resolved shear stress (τ) for each slip system (s).
- Equation between strain rate $\dot{\varepsilon}_{ij}(x)$ and the deviatoric stress $\sigma'(x)$ is given by:



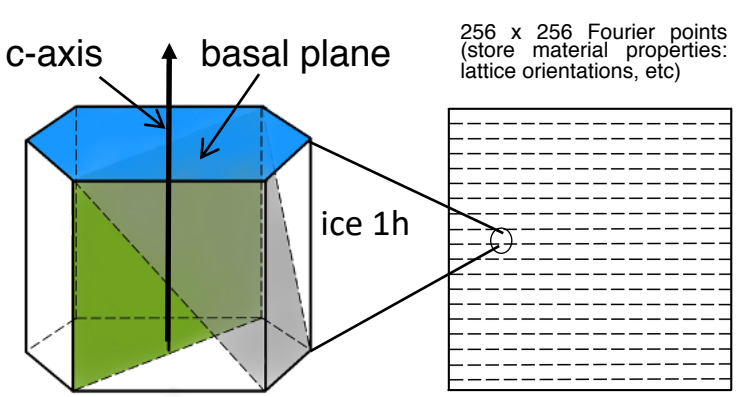
$$\dot{\varepsilon}_{ij}(\boldsymbol{x}) = \sum_{s=1}^{N_s} m_{ij}^s(\boldsymbol{x})\dot{\gamma}^s(\boldsymbol{x}) = \dot{\gamma}_0 \sum_{s=1}^{N_s} m_{ij}^s(\boldsymbol{x}) \left| \frac{m_{ij}^s(\boldsymbol{x}) : \sigma_{ij}'(\boldsymbol{x})}{\tau_0^s(\boldsymbol{x})} \right|^n \operatorname{sgn}\left\{ m_{ij}^s(\boldsymbol{x}) : \sigma_{ij}'(\boldsymbol{x}) \right\}$$

- Strain rate is the sum of simple shearing parallel to each slip system
- Each slip system has its own viscous resistance (τ) to shearing
- Material has a power-law relationship between stress and strain rate ($n = 3$)

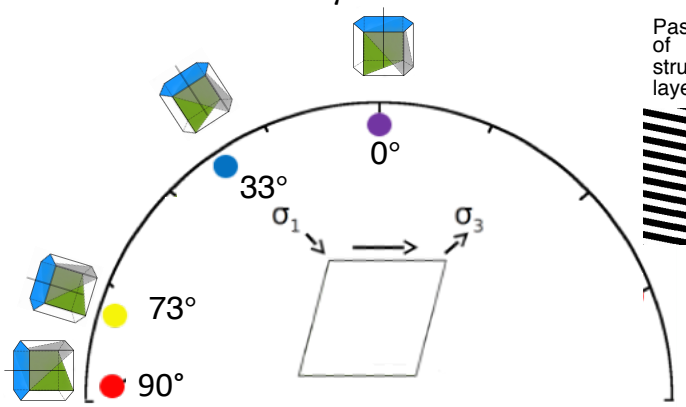
de Riese, T., Bons, P. D., Gomez-Rivas, E., Griera, A., Llorens, M.-G., and Weikusat, I.: Deformation structures resulting from anisotropy during high-strain deformation of ice 1h with initial CPO, EGU General Assembly 2021, online, 19–30 Apr 2021, EGU21-10209, https://doi.org/10.5194/egusphere-egu21-10209, 2021.

Modelling approach: VPFFT + ELLE

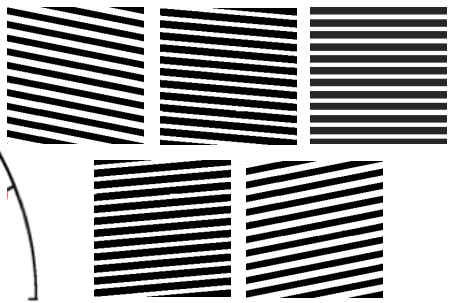
- FFT calculates stress and strain rate field for all grid points and provides velocity field (used for visualisation)
- Ice Ih used as model material. Each point in the model box represents a single grain with a constant internal crystal orientation
- Intrinsic Anisotropy $A = \frac{\tau_{(non-basal)}}{\tau_{(basal)}} = 64$ (ratio of critical resolved shear stresses for basal and non-basal slip)
- **Investigate:**
  - **Effect of a pre-existing crystallographic preferred orientation ($\pm 5°$ noise) on localisation and deformation behaviour**
  - **The role of passive material markers (cloudy bands) in the development of deformation structures**
- Simple shear deformation up to very high strains ($\gamma = 30$, corresponding to a displacement by 6km of the top of a basal shear layer of 200m thickness), with shear-strain increments of $\gamma = 0.02$



256 x 256 Fourier points (store material properties: lattice orientations, etc)

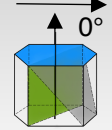


Passive markers (layers) are used on top of the model to visualize deformation structures (as an analogue to stratigraphic layers in ice)



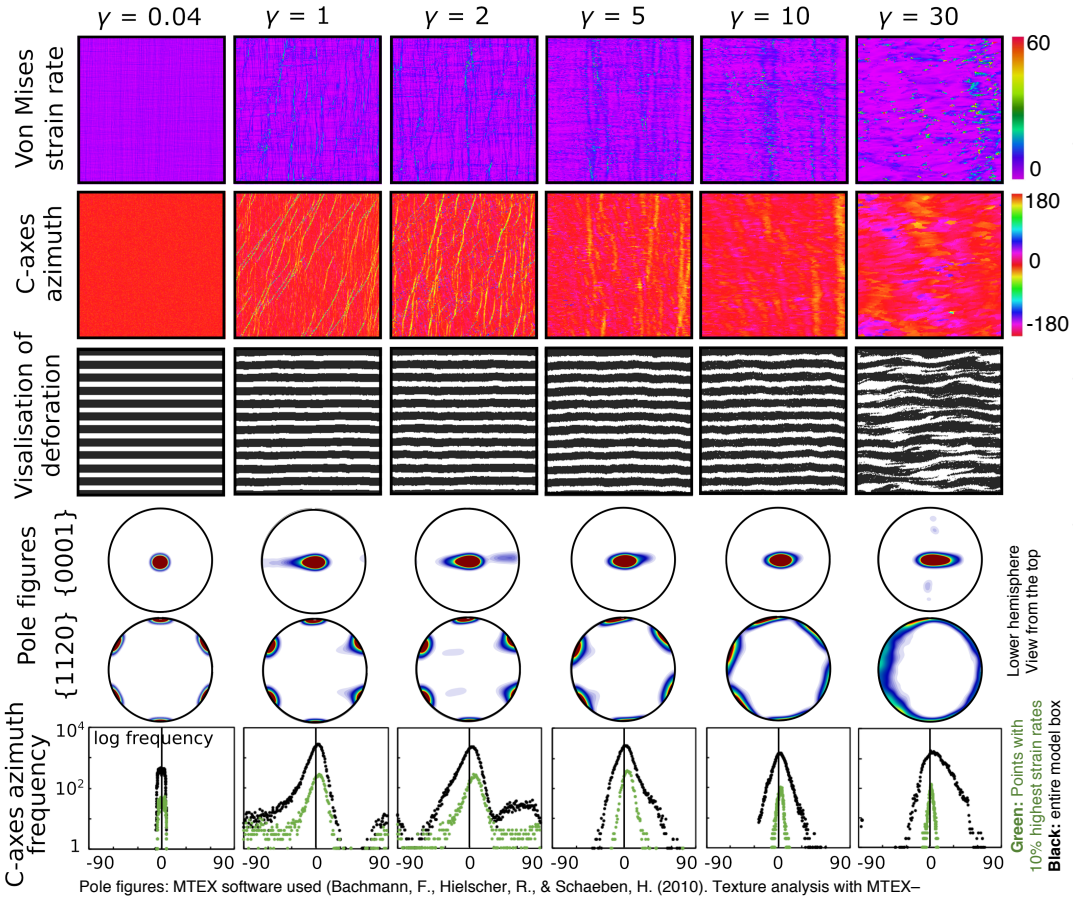
de Riese, T., Bons, P. D., Gomez-Rivas, E., Griera, A., Llorens, M.-G., and Weikusat, I.: Deformation structures resulting from anisotropy during high-strain deformation of ice 1h with initial CPO, EGU General Assembly 2021, online, 19–30 Apr 2021, EGU21-10209, https://doi.org/10.5194/egusphere-egu21-10209, 2021.

Case 1: Distributed localisation



Initial c-axis orientation perpendicular to the shear plane (azimuth = 0°)

-> basal planes parallel to shear direction

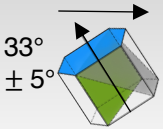


Pole figures: MTEX software used (Bachmann, F., Hielscher, R., & Schaeben, H. (2010). Texture analysis with MTEX–free and open source software toolbox. In *Solid State Phenomena* (Vol. 160, pp. 63-68). Trans Tech Publications Ltd.)

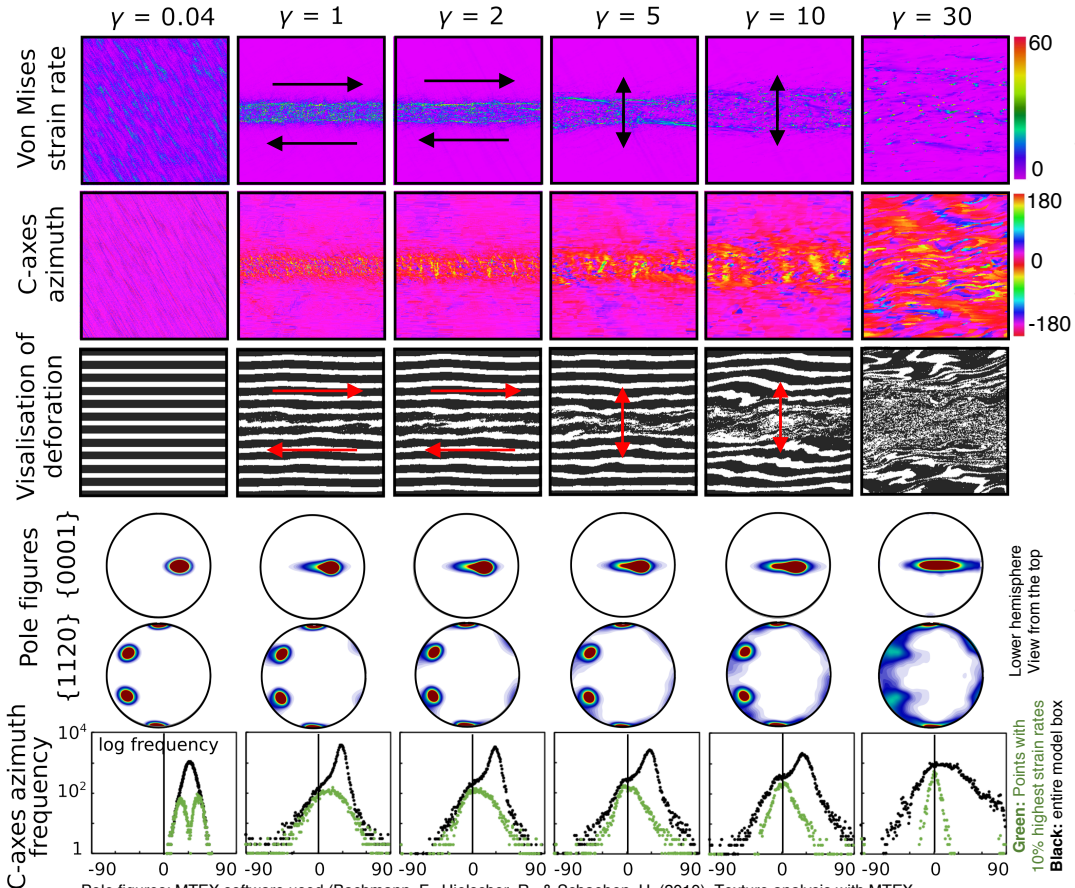
- Conjugate set of high strain rate zones develops. After a shear strain of $\gamma = 30$ patches of high strain rate zones remain.
- C-axis distribution shows kinked bands for low strains. After a shear strain of $\gamma = 30$ zones with differing orientations have been developed, whereas in the biggest part of the model box c-axes are perpendicular to the shear plane.
- C-axes azimuth frequency distributions: Widening of c-axis distribution for low strains, then narrowing again.
- With layers parallel to the shear plane and initial basal planes a huge amount of strain is needed to see deformation structures.

de Riese, T., Bons, P. D., Gomez-Rivas, E., Griera, A., Llorens, M.-G., and Weikusat, I.: Deformation structures resulting from anisotropy during high-strain deformation of ice 1h with initial CPO, EGU General Assembly 2021, online, 19–30 Apr 2021, EGU21-10209, https://doi.org/10.5194/egusphere-egu21-10209, 2021.

Case 2: Synthetic shear zone



Initial c-axis orientation rotated by 33° (azimuth = 33°)

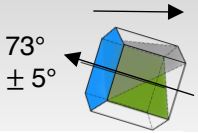


Pole figures: MTEX software used (Bachmann, F., Hielscher, R., & Schaeben, H. (2010). Texture analysis with MTEX–free and open source software toolbox. In *Solid State Phenomena* (Vol. 160, pp. 63-68). Trans Tech Publications Ltd.)

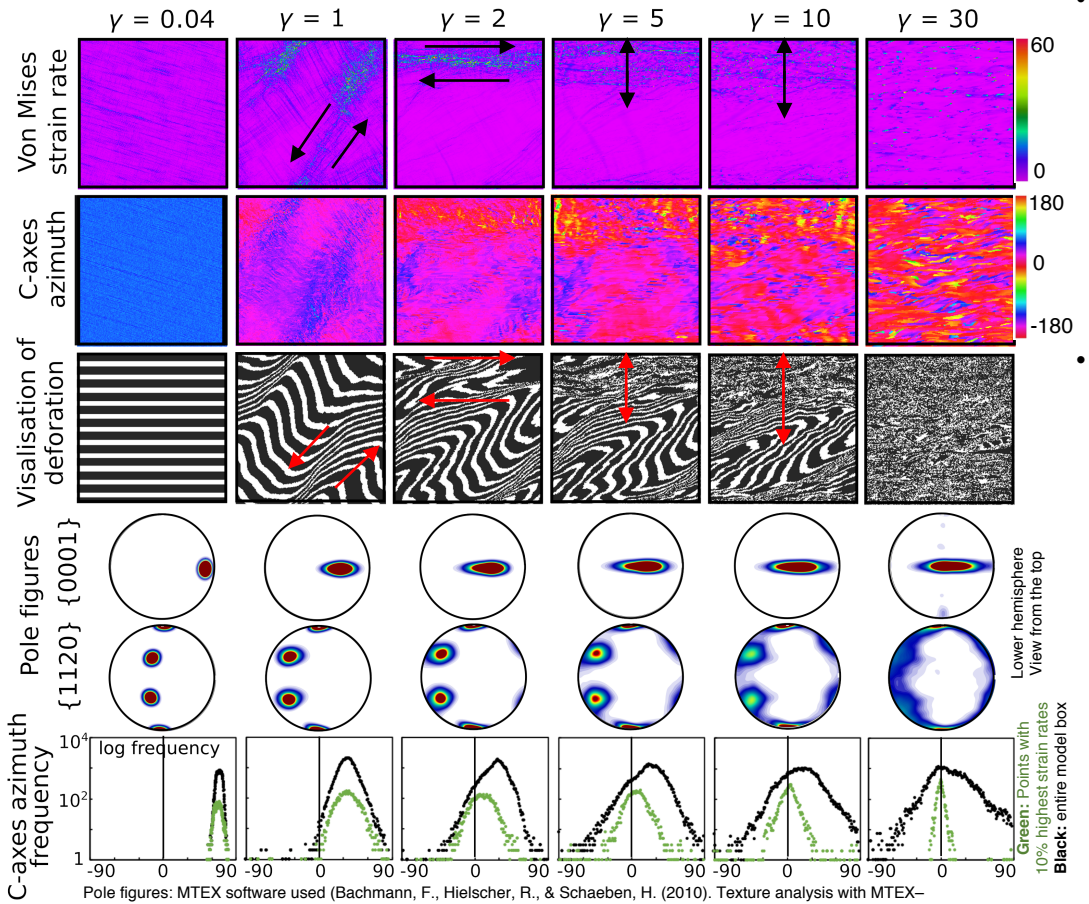
- During the first steps development of high strain rate zones perpendicular to basal planes. C-axis azimuth distribution shows the same pattern.
- Then a synthetic high strain rate zone develops, which is relatively stable. Widens with ongoing strain until it fully collapsed at a shear strain of $\gamma = 30$.
- Most basal planes in high strain rate zones rotate into the shear direction, whereas rotation is slower in the less deformed area. Already after a shear strain of $\gamma = 2$ basal planes in high strain rate zones are oriented mostly parallel to the shear direction. In the entire model box where strain rates are less high zones develop where basal planes are rotated into both directions.
- When using layers parallel to the shear direction deformation structures become apparent after a shear strain of $\gamma = 5 - 10$. Before the layers in the high strain rate zones are slightly wavy. When the high strain rate zone widens deformation becomes obvious, with mixing in the high strain rate zone and folding in adjacent and less deformed areas.

de Riese, T., Bons, P. D., Gomez-Rivas, E., Griera, A., Llorens, M.-G., and Weikusat, I.: Deformation structures resulting from anisotropy during high-strain deformation of ice 1h with initial CPO, EGU General Assembly 2021, online, 19–30 Apr 2021, EGU21-10209, https://doi.org/10.5194/egusphere-egu21-10209, 2021.

Case 3: antithetic + synthetic shear bands



Initial c-axis orientation rotated by 73° (azimuth = 73°)

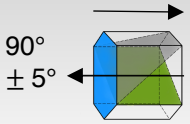


Pole figures: MTEX software used (Bachmann, F., Hielscher, R., & Schaeben, H. (2010). Texture analysis with MTEX–free and open source software toolbox. In *Solid State Phenomena* (Vol. 160, pp. 63-68). Trans Tech Publications Ltd.)

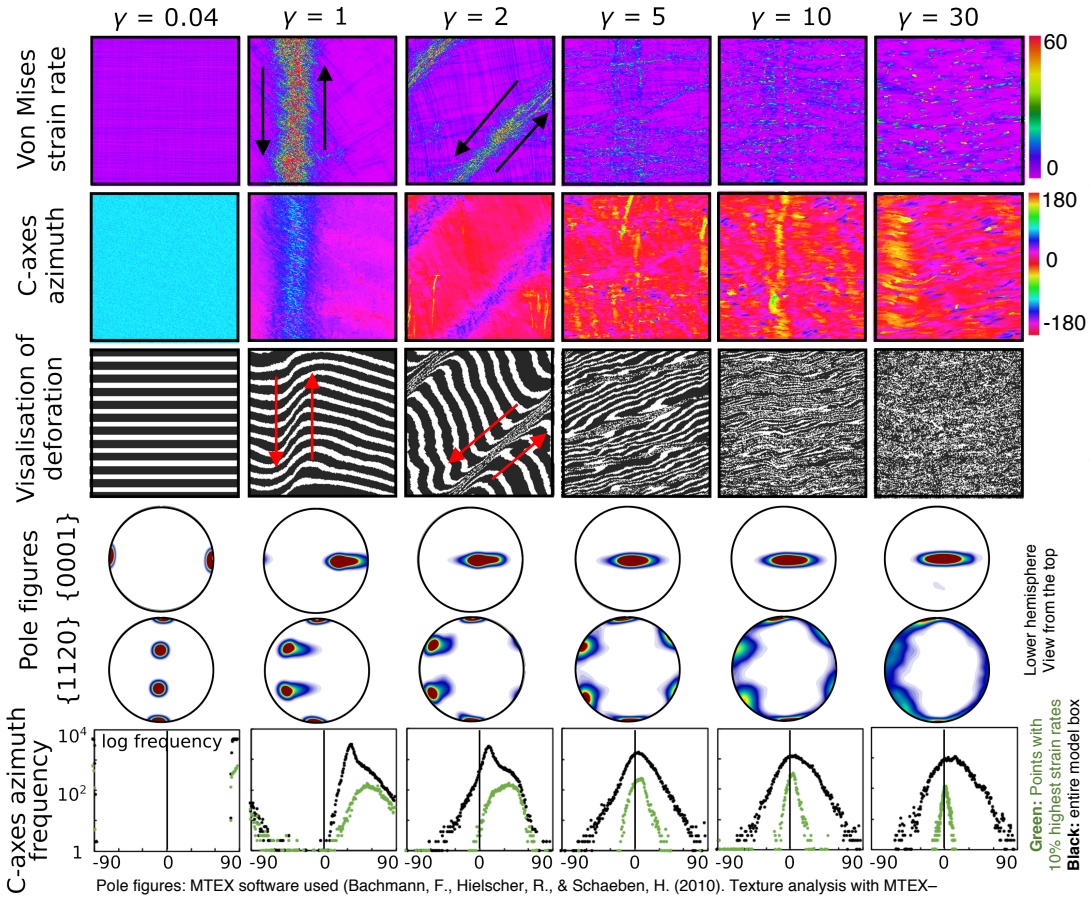
- For low strains a rotating antithetic high strain rate zone develops, which then gets overprinted by a synthetic high strain rate band ($\gamma = 2$). Equivalent structures develop in the layer visualisation. The synthetic high strain rate bands start to dissolve at $\gamma = 5$, when the visual shear band starts to widen. After a shear strain of $\gamma = 30$ the material is strongly mixed.
- Again, basal planes in the high strain rate zones rotate faster into the shear direction in comparison to basal planes in the entire model box. After a shear strain of $\gamma = 30$ the frequency distribution of c-axis azimuths is relative wide compared to high strain rate areas (as in all cases).

de Riese, T., Bons, P. D., Gomez-Rivas, E., Griera, A., Llorens, M.-G., and Weikusat, I.: Deformation structures resulting from anisotropy during high-strain deformation of ice 1h with initial CPO, EGU General Assembly 2021, online, 19–30 Apr 2021, EGU21-10209, https://doi.org/10.5194/egusphere-egu21-10209, 2021.

Case 4: Antithetic shear bands



Initial c-axis orientation rotated by 90° (azimuth = 90°)

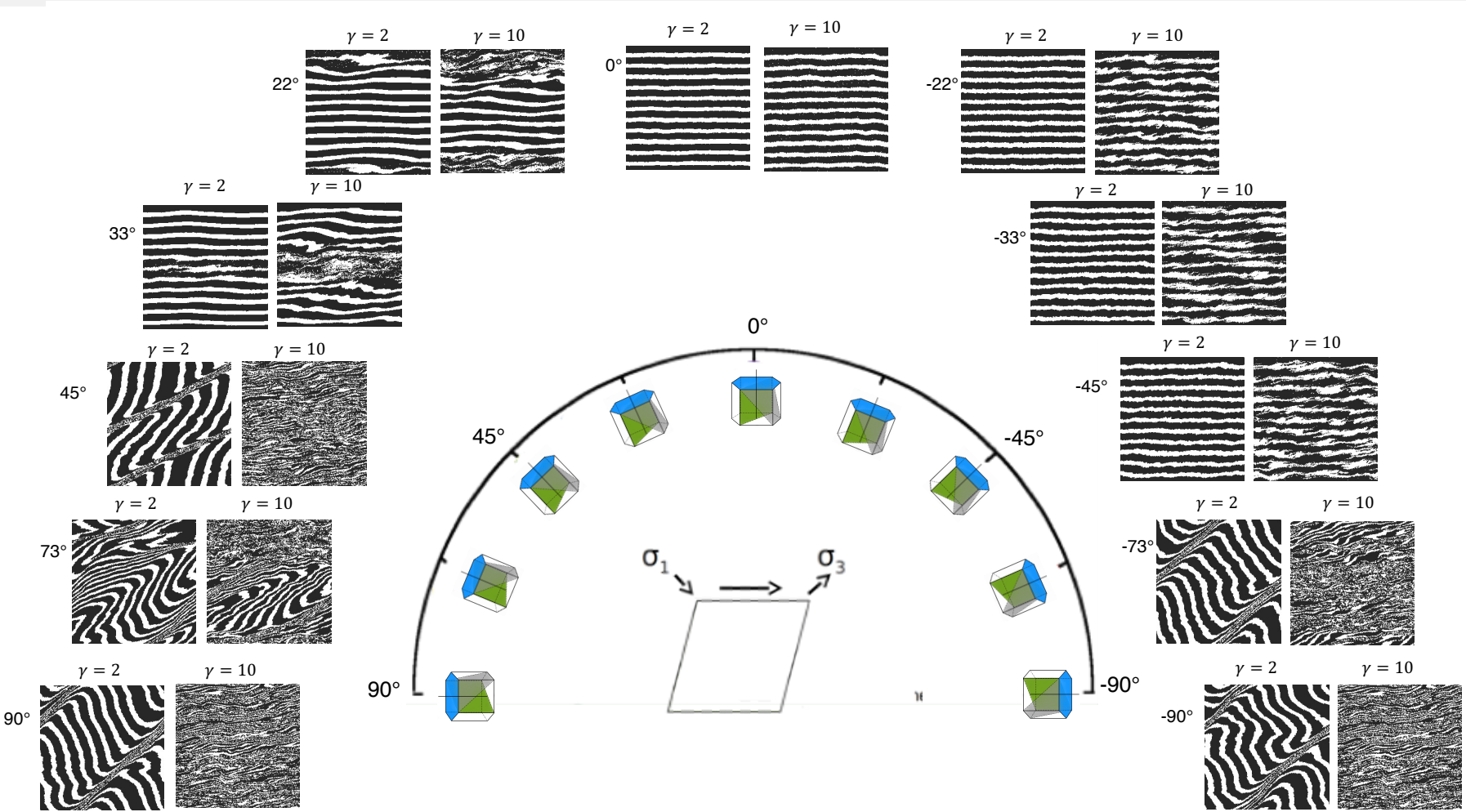


Pole figures: MTEX software used (Bachmann, F., Hielscher, R., & Schaeben, H. (2010). Texture analysis with MTEX–free and open source software toolbox. In *Solid State Phenomena* (Vol. 160, pp. 63-68). Trans Tech Publications Ltd.)

- For low strains rotating antithetic high strain rate zones develops, which already dissolve after a shear strain of $\gamma = 2$. Afterwards the von Mises strain rate field shows distributed localisation.
- Compared to case 2 and 3, deformation (the antithetic shear band) becomes visible relatively late. Basal planes first need to reorient, then the localisation starts. After a shear strain of $\gamma = 5$ layers are stretched, afterwards the material is mixed.
- In this case the frequency distribution of c-axis azimuths for points in the model box with highest strain rates rotates slower than points in the entire model box. After a shear strain of $\gamma = 5$ all basal planes are oriented approx. parallel to the shear direction. Again, the frequency distribution of c-axis azimuths for points with highest strain rates is quite narrow, whereas the distribution in the entire model box is relatively wide.

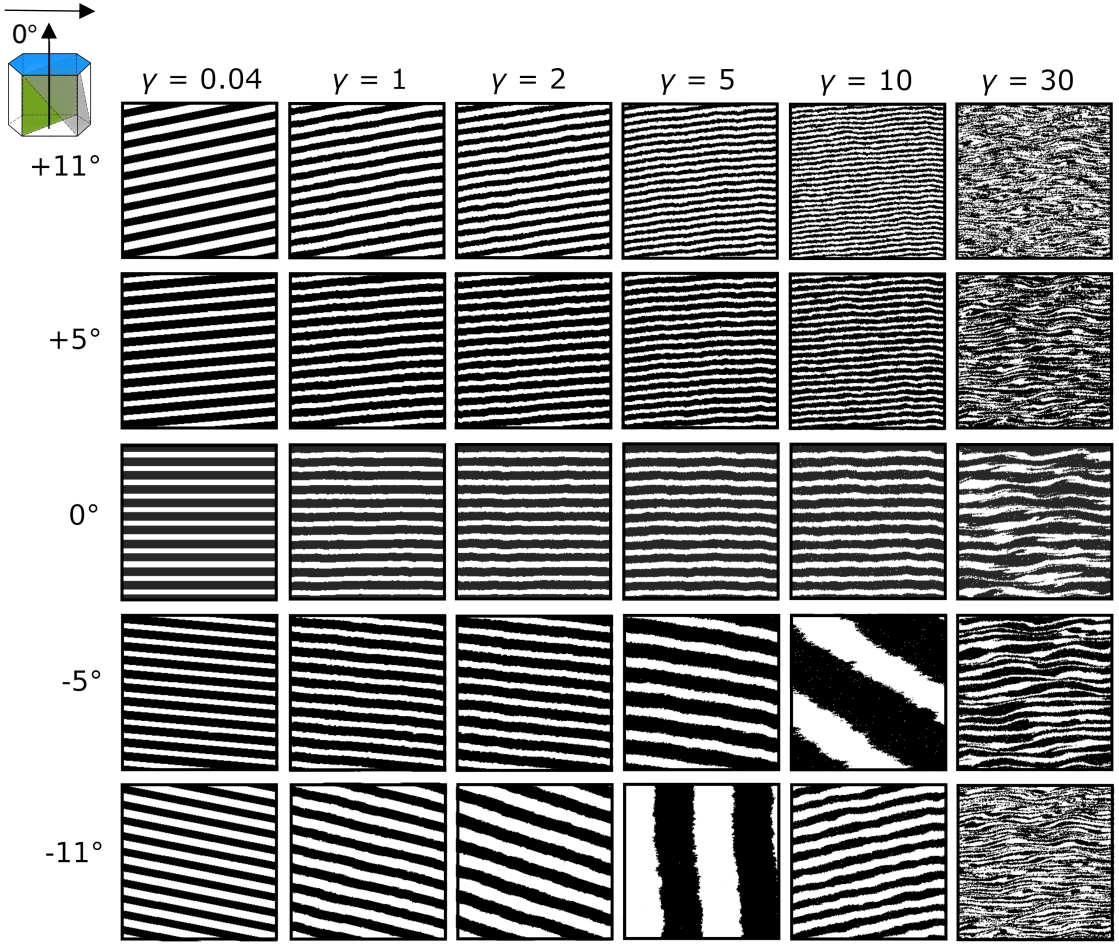
de Riese, T., Bons, P. D., Gomez-Rivas, E., Griera, A., Llorens, M.-G., and Weikusat, I.: Deformation structures resulting from anisotropy during high-strain deformation of ice 1h with initial CPO, EGU General Assembly 2021, online, 19–30 Apr 2021, EGU21-10209, https://doi.org/10.5194/egusphere-egu21-10209, 2021.

Deformation structures depending on initial CPO with horizontal layering



de Riese, T., Bons, P. D., Gomez-Rivas, E., Griera, A., Llorens, M.-G., and Weikusat, I.: Deformation structures resulting from anisotropy during high-strain deformation of ice 1h with initial CPO, EGU General Assembly 2021, online, 19–30 Apr 2021, EGU21-10209, https://doi.org/10.5194/egusphere-egu21-10209, 2021.

Importance of inclination/orientation of cloudy bands

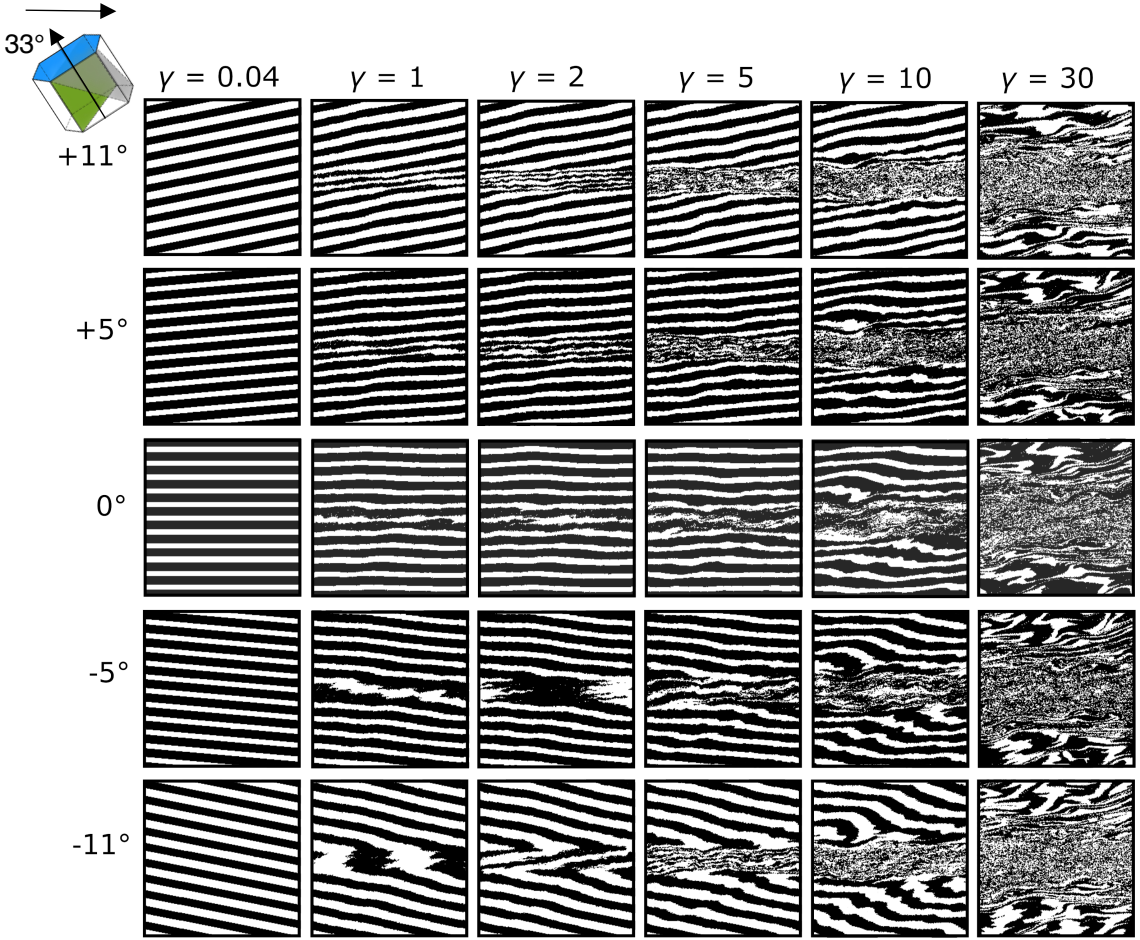


Case 1 (distributed localisation with initial c-axis azimuth of 0°)

- With horizontal layers deformation structures become visible only after very high strains.
- Using slightly different starting orientations/inclinations of the layering has a huge influence on the development of deformation structures.
- With inclinations of -5° and -11° layers rotate and first thicken, then stretch.
- With inclinations of 5° and 11° layers stretch and become thinner.

de Riese, T., Bons, P. D., Gomez-Rivas, E., Griera, A., Llorens, M.-G., and Weikusat, I.: Deformation structures resulting from anisotropy during high-strain deformation of ice 1h with initial CPO, EGU General Assembly 2021, online, 19–30 Apr 2021, EGU21-10209, https://doi.org/10.5194/egusphere-egu21-10209, 2021.

Importance of inclination/orientation of cloudy bands

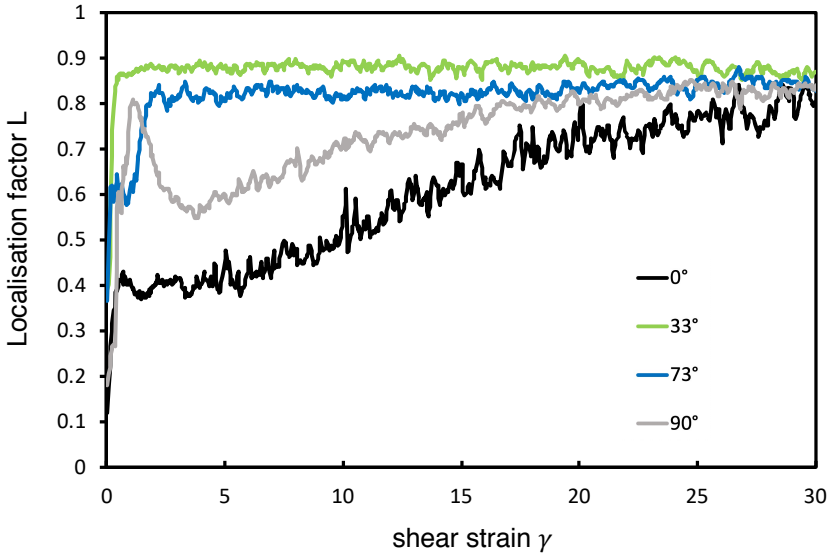


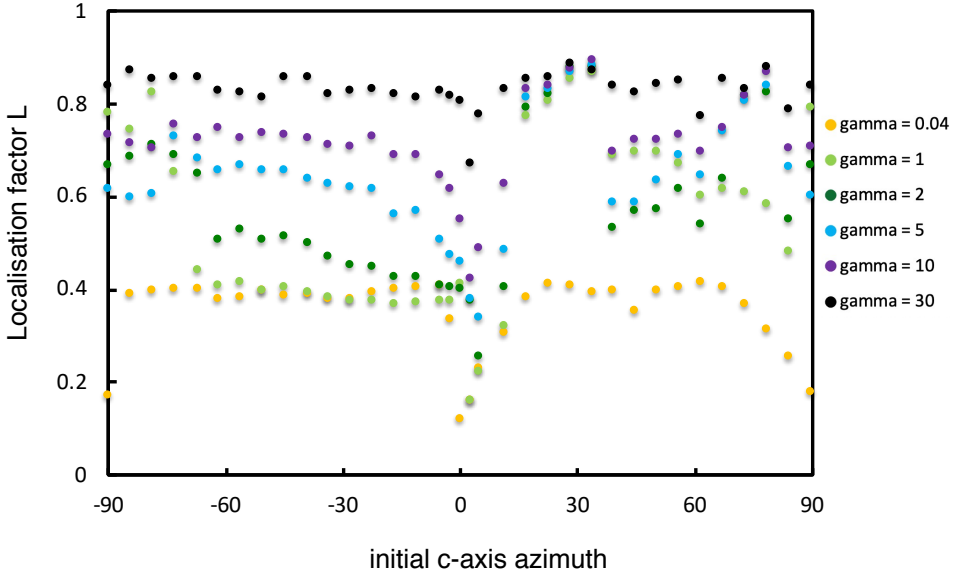
Case 2 (synthetic localisation with initial c-axis azimuth of 33°)

- With horizontal layers deformation structures become visible only after high strains.
- With inclinations of 5° and 11° layers in the high strain rate zone become stretched, because of that the shear zones becomes visible relatively early.
- With inclinations of -5° and -11° layers in the high strain rate zone thicken and folds develop.
- After a shear strain of $\gamma = 30$ the overall picture of deformation is quite similar, but for lower strains deformation structures are highly variable.

de Riese, T., Bons, P. D., Gomez-Rivas, E., Griera, A., Llorens, M.-G., and Weikusat, I.: Deformation structures resulting from anisotropy during high-strain deformation of ice 1h with initial CPO, EGU General Assembly 2021, online, 19–30 Apr 2021, EGU21-10209, https://doi.org/10.5194/egusphere-egu21-10209, 2021.

localisation of strain rates





- Strain rate localisation has been quantified with a localisation factor (see equation). $L = 0$ denotes homogeneous localisation, $L = 1$ denotes maximum localisation.
- For low strains localisation behaviour depends on the initial CPO. After $\gamma = 30$ all cases reach a consistent state with strong strain rate localisation. Localisation behaviour of simulations with the same deformation behaviour evolve with a similar trend.

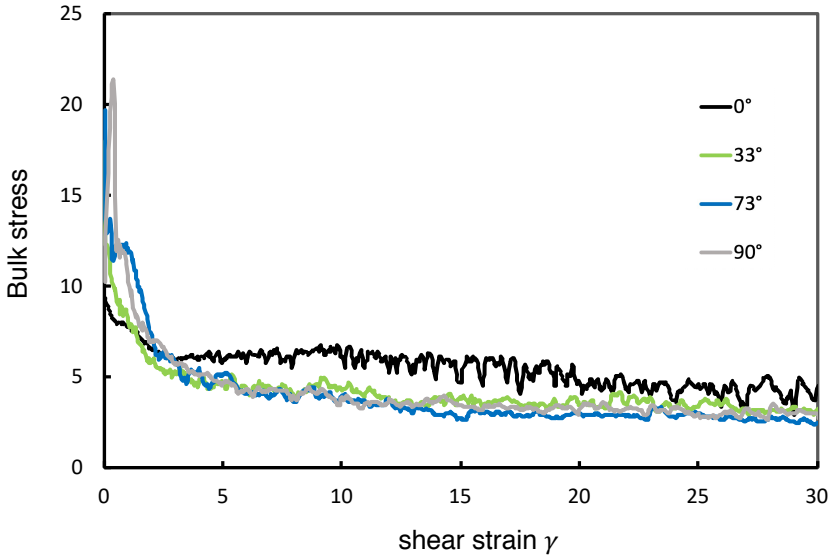
$$L = 1 - \frac{\left(\sum_{n_i}^{n_i} \dot{\varepsilon}_{VM}\right)^2}{n_i \sum_{n_i}^{n_i} \left(\dot{\varepsilon}_{VM}\right)^2},$$

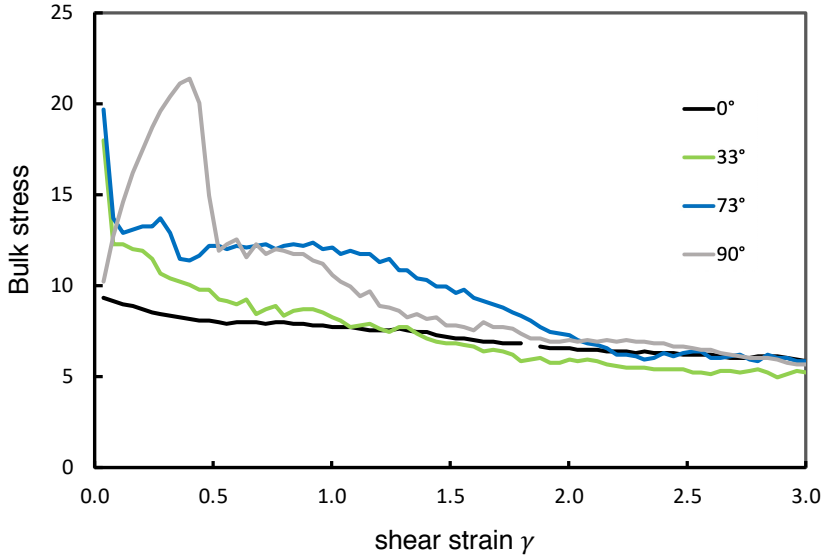
Calculation: Defined by Sornette et al., (1993) and Davy et al. (1995), modified by Gomez-Rivas (2008)

Gómez Rivas, E., 2008. Localización de deformación en medios dúctiles y anisótropos. Unpublished PhD-thesis, Universitat Autònoma de Barcelona.
Davy, P., Hansen, A., Bonnet, E., Zhang, S.Z., 1995. Localization and fault growth in layered brittle-ductile systems: Implications for deformations of the continental lithosphere. Journal of Geophysical Research: Solid Earth, 100, 6281-6294.
Sornette, A., Davy, P., Sornette, D., 1993. Fault growth in brittle-ductile experiments and the mechanics of continental collisions. Journal of Geophysical Research: Solid Earth, 98, 12111-12139

de Riese, T., Bons, P. D., Gomez-Rivas, E., Griera, A., Llorens, M.-G., and Weikusat, I.: Deformation structures resulting from anisotropy during high-strain deformation of ice 1h with initial CPO, EGU General Assembly 2021, online, 19–30 Apr 2021, EGU21-10209, https://doi.org/10.5194/egusphere-egu21-10209, 2021.

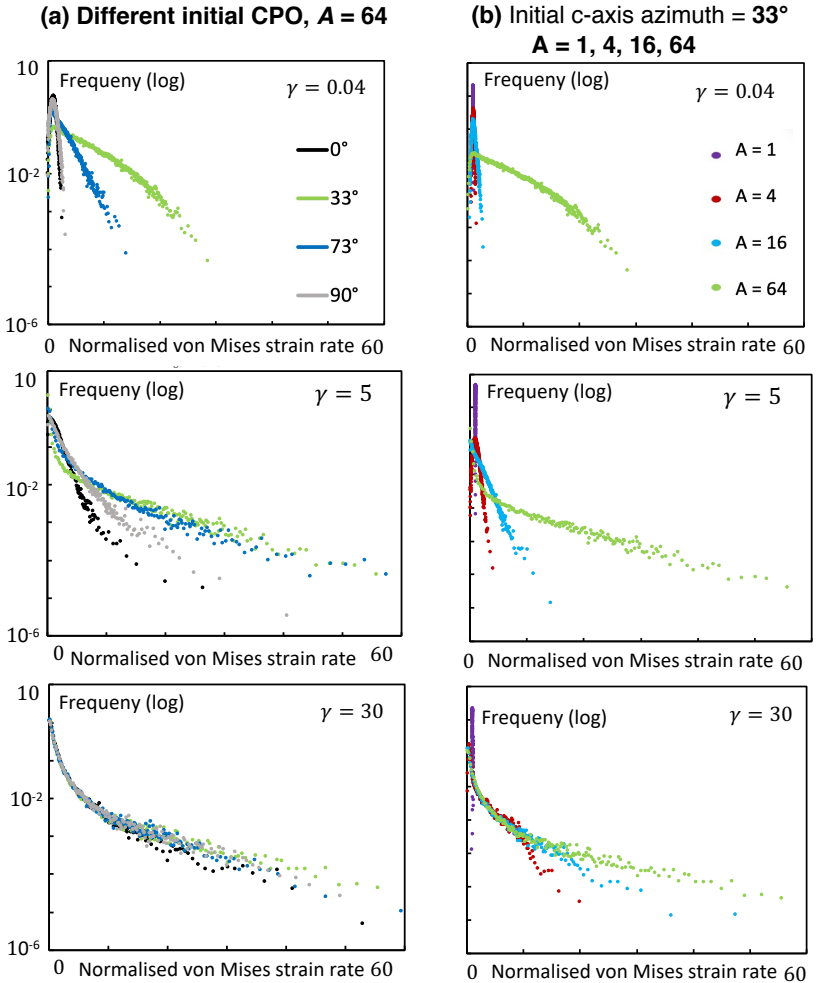
Evolution of bulk von Mises stress





de Riese, T., Bons, P. D., Gomez-Rivas, E., Griera, A., Llorens, M.-G., and Weikusat, I.: Deformation structures resulting from anisotropy during high-strain deformation of ice 1h with initial CPO, EGU General Assembly 2021, online, 19–30 Apr 2021, EGU21-10209, https://doi.org/10.5194/egusphere-egu21-10209, 2021.

Frequency of von Mises strain rates



- (a) shows the frequency distributions of strain rates for the four cases with different initial CPOs. In cases where the ice immediately localises, the frequency distribution becomes heavy tailed (high strain rate values become overrepresented). In case 1 (0°, distributed localisation) and 4 (antithetic shear bands), which both develop deformation structures and a high localisation factor relatively late, the frequency distribution of strain rates is approx. normal distributed for low strains.
- (b) shows a series with a CPO as in case 2 (33°), but now with different A (Anisotropy). $A = 1$ and $A = 4$, (isotropic and minimal anisotropic), produces normal distributions. When using $A > 1$ the frequency distributions become heavy tailed after a shear strain of $\gamma = 30$, but not as much as when $A = 64$ is used. Simulation results of series (b) ($A = 1$, 4 and 16) are not shown in this presentation, but develop a distributed kind of localisation, what happens as well when starting with a random c-axis distribution (de Riese et al., 2019).
- With $A = 64$ the frequency distributions of normalised von Mises strain rates become power law distributed after very high strains (a). A material with a high degree of anisotropy + a certain CPO reaches quite high strain-rate values due to strain localisation.
- As has been seen in a previous study, the shape of strain rate frequency distributions in anisotropic ice is largely independent of the size of the model box (de Riese et al., 2019). When using a model box with double the length of a model box side, the probability to reach a particular strain rate is four times higher. Therefore it can be assumed that strain rate localisation happens on all scales.

de Riese, T., Evans, L., Gomez-Rivas, E., Griera, A., Lebensohn, R. A., Llorens, M. G., ... & Bons, P. D. (2019). Shear localisation in anisotropic, non-linear viscous materials that develop a CPO: A numerical study. *Journal of Structural Geology*, *124*, 81-90.

de Riese, T., Bons, P. D., Gomez-Rivas, E., Griera, A., Llorens, M.-G., and Weikusat, I.: Deformation structures resulting from anisotropy during high-strain deformation of ice 1h with initial CPO, EGU General Assembly 2021, online, 19–30 Apr 2021, EGU21-10209, https://doi.org/10.5194/egusphere-egu21-10209, 2021.

Summary and conclusions

- Anisotropy and the orientation of an initial CPO controls the style of deformation.
- At relatively low strains the amount of strain rate localisation and resulting deformation structures depend on the initial CPO in the anisotropic material.
- Four regimes can be recognised: (1) Distributed shear localisation, (2) synthetic shear bands (widening with ongoing strain until it collapses), (3) antithetic shear bands (rotating and relatively unstable), and (4) first antithetic shear bands, which get overprinted by a synthetic shear band. However, after very high strains the material reaches a consistent state and is almost always strongly mixed.
- Visual layering/stratigraphy such as cloudy bands are the essential feature of polar ice to identify deformation structures, as ice otherwise has no markers.
- Small changes in the layer orientation/inclination can lead to different visible deformation structures.
- After very high strains, localisation behaviour, fabric evolution, evolving structures, etc. reach a consistent state, but need different amounts of strain to reach this state and show variable evolutions for low strains.
- The long deformation history of flowing ice and the fact that ice layers are possibly strongly mixed makes it difficult to use deep ice cores for climate reconstructions.
- As strain localisation in ice behaves scale-independent, large-scale equivalents of the observed small-scale structures may occur.

de Riese, T., Bons, P. D., Gomez-Rivas, E., Griera, A., Llorens, M.-G., and Weikusat, I.: Deformation structures resulting from anisotropy during high-strain deformation of ice 1h with initial CPO, EGU General Assembly 2021, online, 19–30 Apr 2021, EGU21-10209, https://doi.org/10.5194/egusphere-egu21-10209, 2021.